Characterization of bulk structure and optical properties of zinc stannate (ZTO)

Grigory Kolesov

Abstract

Zn_2SnO_4(ZTO) is an important material with a wide bandgap. It is often used in nano devices such as solar cells. The crystal structure of ZTO is inverse spinel, with the general formula AB_2O_4. In inverse spinel the occupation of the octahedral sites is not determined, but instead A and B atoms share the occupation 50/50. Here we elaborate on the previous computational work done on this material using DFT, cluster expansion and Monte Carlo calculation of a phase diagram. This is the research-in-progress and the results are not final.

1 Methods

The preliminary scan of configuration space of ZTO was performed using SIESTA[1] code with T-M pseudopotenials. Further calculations on the ground state structure were done using QuantumEspresso[2] code with PBE functional. Bether-Salpeter equation (BSE) is being solved with YAMBO code[3]. Unless otherwise stated, ZTO was represented by a 56-atom unit cell; $5\times5\times5$ Γ-centered k-point mesh was used in the calculations that involved geometry relaxation.

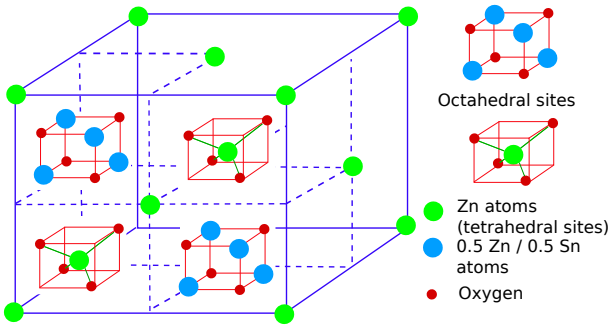

Figure 1: Schematic structure of inverse spinel ZTO. Atoms in blue represent 0.5/0.5 mixture of Zn/Sn atoms. Atoms in green are Zn atoms that occupy tetrahedral (diamond-like) sites on the lattice.

We used ATAT code [4–8] to generate special quasy random structure (SQS) [9,10], to conduct cluster expansion (CE) and to perform Monte Carlo simulations. We used SIESTA with LDA functional and $5 \times 5 \times 5$ k-point mesh as an *ab initio* input for ATAT to perfrom CE. We may remark here that speed-up benefits from SIESTA are very significant in comparison to other popular solid-state codes, the fact that comes extremely useful in situations when many configurations of large unit cell must be sampled.

ZTO crystall structure is known as inverse spinel. Oxide spinels, such as ZTO are represented by a general stoichiometric formula AB_2O_4. Such spinels exist in two forms , 2-3 form where A is ionized to +2e charge and B to +3e; and 4-2 form where A carries +4e and B +2e charges. ZTO corresponds to the latter form. More generally, all AB_2O_4 spinels can be described by degree of inversion, x, using the formula $(A_{1-x}B_x)[A_xB_{2-x}]O_4$. Here the parenthesis () refer to tetrahedral (diamond-like) sites and brackets [] refer to octahedral sites. Consequently $x = 0$ corresponds to the normal spinel structure and $x = 1$ to inverse.

In the X-ray diffraction (XRD) experiments [11] on bulk ceramic ZTO the space group $Fd3m$ (227) was identified, and the degree of inversion x was found to be 0.99. The inverse spinel structure is shown on Fig. 1. The XRD

experiments however could not resolve the exact occupation of the octahedral sites, which were are assigned to be 0.5/0.5 Sn/Zn occupied (hence the space group). In the previous computational work on ZTO[12,13] the occupation of these sites was assumed to be random.

Similiar problems were encountered in studies of bulk Zn_2TiO_4[14] (we will abreviate this material as TiZO to avoid confusion). TiZO has also been found to have inverse spinel structure with XRD assigned 0.5/0.5 occupation of tetrahedral sites. Hovewer recent results of Extended X-Ray Absorption Fine Structure (EXAFS) experiments when compared with results of DFT and Monte Carlo simulations found that the symmetry-degenerate ground state configurations are the most likely candidates for the room temperature configuration of bulk TiZO.[15] the difference of experimental lattice constants within 0.2 Å (8.48Å for TiZO and 8.65Å for ZTO).

To describe configurations we used notation from the latter article[15]. Four principal points[14] corresponding to Zn/Sn octahedral sites are denoted as 1a, 1b, 1c, 1d and the other 12 points (2a, 2b, ..., 4d) are generated from them by the standard fcc space group operators[15].

2 Results

The goal of the first stage the calculation is to compare our results with previous work done on ZTO and TiZO[12,13,15]. In the first two articles authors assume random order of Zn and Sn atoms and use SQS for calculations. In the last reference a ground state configuration is found for TiZO and it is shown, with some supporting experimental evidences, that it dominates the bulk for temperatures $<$700K .

We first verified the assumption that ground state configuration for ZTO matches that of TiZO . To do this we selected 6 top lowest energy configurations described for TiZO[15]. The results are summarized in Table 1. Indeed

the ground state denoted as 1a,1b,2c,2d,3a,3b,4c,4d for ZTO had the lowest energy among these 10 configurations. The ordering of the other configurations sorted by the energy didn't match that of TiZO. Thus we can conclude that we can not directly map configurational properties of TiZO to ZTO and further studies of configurational space of ZTO are required.

Table 1: Comparison of the first 6 configurations of ZTO and TiZO. First two configurations are symmetry-degenerate. Energies are relative to the ground state and are per atom.

Configuration	ZTO Energy, eV	lattice constant, Å	TiZO Energy, eV
1a,1b,2c,2d,3a,3b,4c,4d	0.0	6.7	0.0
1b,1c,2a,2d,3b,3c,4a,4d	0.0	6.7	0.0
1b,2a,3a–d,4c,4d	3.2	6.75	0.52
1d,2a,2b,2c,3b,3c,3d,4a	2.2	6.7	0.58
1a,1c–2c,3a,4b	3.1	6.75	0.58
1a,1b,1c,2d,3a,4b,4c,4d	2.3	6.7	0.58

2.1 Cluster Expansion method

It is necessary to know, what configuration, if any, is dominant in a ZTO sample at the normal range of temperatures. In order to answer this question we build the cluster expansion (CE)[16] with ATAT code and performed Monte Carlo (MC) simulations.

CE is a method to study a configuration space of an alloy. It does not calculate each point by an *ab initio* method, which is unfeasible in most cases, but instead employes interpolation. In CE the energy is expanded into a series of correlation functions $\langle \Pi_\alpha \rangle$ for clusters α of lattice sites (single atoms, pairs, triplets, etc):

$$E = \sum_\alpha J_\alpha m_\alpha \langle \Pi_\alpha \rangle$$

Here m_α are degeneracy factors due to the symmetries and J_α are coeffi-

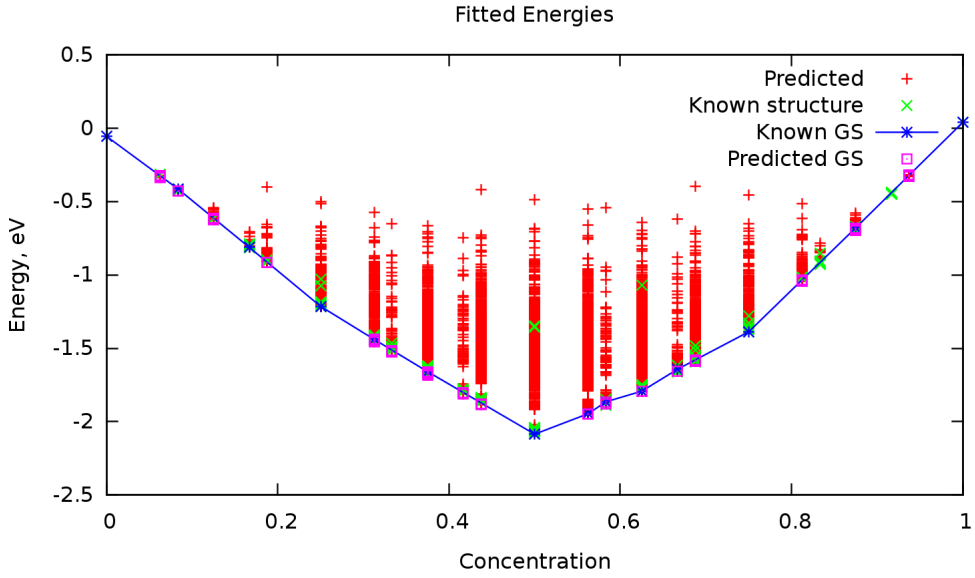

Figure 2: CE energies for various configurations at different concentrations (different chemical potential difference μ). The error of CE fit is $<$0.01 eV for 0.5 concentration. GS refers to the ground state configurations.

cients found by CE by fitting configurations with known energies (calculated by an *ab initio* method). In binary systems, such as ZTO, cluster function Π_α is simply a product of fictitious spin ± 1 variables (designating A/B atoms) assigned to the corresponding lattice sites. CE can be generalized to multicomponent systems.[6,16] CE is known to converge quickly and this is a singular advantage of this expansion.

We ran ATAT starting from the spinel (fcc) primitive unit cell composed of 14 atoms. Before it converged (cross-validation score $<$0.025 *eV)* the unit cell was extended upto the 56-atom unit cell.

ATAT studies the whole composition space of an alloy. The plot of fitted energies versus composition is presented on Fig.2. As expected from experimental data, the lowest energy configurations belong to 0.5/0.5 Sn/Zn composition of octahedral sites.

ATAT-predicted ground state configuration for 0.5 concentration matched an $(\infty, 0, \infty)$ reflection of configuration 1 (Table 1), *i.e.* these two configurations are degenerate. No lower energy configurations with different Zn/Sn composition was predicted by ATAT.

2.2 Monte Carlo simulation

Given the CE expansion it is feasible to study thermodynamic properties of alloys with MC method. For thermodynamic description of alloys semi-grand-canonical ensemble is usually employed. In this ensemble the total number of particles N is kept constant, while the concentrations of components are allowed to fluctuate. The thermodynamic potential associated with the semi-grand-canonical ensemble is given by

$$\phi(\beta, \mu) = -\frac{1}{\beta N} ln \left(\sum_i exp\left[-\beta N(E_i - \mu a_i)\right] \right) \tag{1}$$

where $\beta = 1/k_B T$ is inverse temperature, $\mu = \mu_A - \mu_B$ is the difference in chemical potentials of the two atom types involved and a_i is a fractional concentration $(0.0 - 1.0)$ of the specie A.

The plot for ZTO energy is presented on Fig.3. Though the whole (β, μ) space can be studied with CE Monte Carlo simulation, the configurations with 0.5/0.5 Sn/Zn concentrations are experimentally relevant for ZTO. Consequently for this simulation the chemical potential μ was kept fixed at a value that stabilizes 0.5/0.5 ground state. This graph demonstrates that the material in the ground state undergoes phase transition at extremely high temperatures of about 3000K. It should be pointed out here, that the energies E_i in 1 are calculated for a fixed lattice without considering motion of the nuclei: at atmospheric pressure the crystal melts at much lower temperatures.

Thus it can be concluded that the ground state configuration for ZTO is

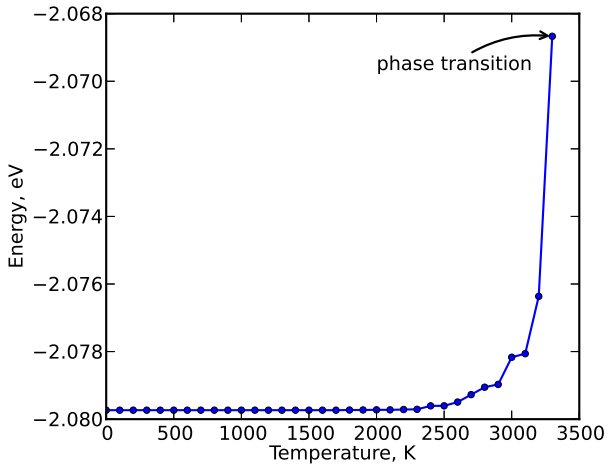

Figure 3: Energy dependence on temperature for ZTO. Energies are normalized to the number of atoms in the unit cell. Phase transition (discontinuity) was detected at the last data point.

remarkably stable.

2.3 Comparison with Special Quasirandom Structure

The properties of ZTO were previously calculated assuming random ordering of Sn and Zn atoms at O sites. To make such computation feasible the SQS approach was introduced. An SQS is simply a cell that generates the same $\langle \Pi_\alpha \rangle$ as for the random structure. This reduces dramatically the size of the supercell needed for calculation. Our prelimary results show that SQS energy is about 2.7 eV higher than that of ground configuration.

Summary

ZTO is a semiconductor alloy material with the complex configuration space. We have studied this configuration space with the cluster expansion method and have found ground state configuration for ZTO. This configuration appear to be thermodynamically stable at all temperatures that ZTO exists.

We have compared ZTO with TiZO - a material with the similar structure and found that while their ground state configuration do coincide, the rest of the configuration space does not. This can be explained by a higher symmetry of the ground state configuration.

Our next goal is to finish calculation of the optical properties of ZTO. This is a difficult task, because the standard DFT computations produce results with the $1 - 2eV$ band gap energy deviation from the experiment. Therefore we employed much more computationally expensive many-body Bethe-Salpeter approach.[3,17]

The final goal of this project is the calculation of configuration and optical properties of ZTO surfaces and surfaces with attached nanostructures.

References

[1] Soler, J. M. *et al.* The siesta method for ab initio order-n materials simulation. *Journal of Physics: Condensed Matter* **14**, 2745 (2002).

[2] Giannozzi, P. *et al.* QUANTUM ESPRESSO: a modular and open-source software project for quantum simulations of materials. *Journal of Physics Condensed Matter* **21**, 5502 (2009).

[3] Marini, A., Hogan, C., Grüning, M. & Varsano, D. Yambo: An ab initio tool for excited state calculations. *Computer Physics Communications* **180**, 1392 – 1403 (2009).

[4] Walle, A. & Ceder, G. Automating first-principles phase diagram calculations. *Journal of Phase Equilibria* **23**, 348–359 (2002).

[5] van de Walle, A., Asta, M. & Ceder, G. The Alloy Theoretic Automated Toolkit: A User Guide. *eprint arXiv:cond-mat/0212159* (2002).

[6] van de Walle, A. Multicomponent multisublattice alloys, nonconfigurational entropy and other additions to the Alloy Theoretic Automated Toolkit. *ArXiv e-prints* (2009).

[7] van de Walle, A. & Asta, M. Self-driven lattice-model Monte Carlo simulations of alloy thermodynamic properties and phase diagrams. *Modelling Simul. Mater. Sci. Eng.* **10**, 521–538 (2002).

[8] Hart, G. L. W. & Forcade, R. W. Algorithm for generating derivative structures. *Phys. Rev. B* **77**, 224115 (2008).

[9] Zunger, A., Wei, S.-H., Ferreira, L. G. & Bernard, J. E. Special quasirandom structures. *Phys. Rev. Lett.* **65**, 353–356 (1990).

[10] Wei, S.-H., Ferreira, L. G., Bernard, J. E. & Zunger, A. Electronic properties of random alloys: Special quasirandom structures. *Phys. Rev. B* **42**, 9622–9649 (1990).

[11] Young, D., Williamson, D. & Coutts, T. Structural characterization of zinc stannate thin films. *JOURNAL OF APPLIED PHYSICS* **91**, 1464–1471 (2002).

[12] Segev, D. & Wei, S.-H. Structure-derived electronic and optical properties of transparent conducting oxides. *Phys. Rev. B* **71**, 125129 (2005).

[13] Wei, S.-H. & Zhang, S. B. First-principles study of cation distribution in eighteen closed-shell $A^{\mathrm{ii}}B_2^{\mathrm{iii}}\mathrm{o}_4$ and $A^{\mathrm{iv}}B_2^{\mathrm{ii}}\mathrm{o}_4$ spinel oxides. *Phys. Rev. B* **63**, 045112 (2001).

[14] Bartram, S. F. & Slepetys, R. A. Compound Formation and Crystal Structure in the System ZnO-TiO2. *Journal of the American Ceramic Society* **44**, 493–499 (1961).

[15] Rankin, Rees B. and Campos, Andrew and Tian, Hanjing and Siriwardane, Ranjani and Roy, Amitava and Spivey, James J. and Sholl, David S. and Johnson, J. Karl. Characterization of Bulk Structure in Zinc Orthotitanate: A Density Functional Theory and EXAFS Investigation. *Journal of the American Ceramic Society* **91**, 584–590 (2008).

[16] Sanchez, J. M., Ducastelle, F. & Gratias, D. Generalized cluster description of multicomponent systems. *Physica A: Statistical Mechanics and its Applications* **128**, 334–350 (1984).

[17] Fetter, A. L. & Walecka, J. D. *Quantum theory of many-particle systems* (Courier Dover Publications, 1971).